

Suppression of multi-pulse formation in all-polarization-maintaining figure-9 erbium-doped fiber mode-locked laser

Jun-Kai Shi(石俊凯), Deng-Feng Dong(董登峰), Ying-Ling Pan(潘映伶), Guan-Nan Li(李冠楠), Yao Li(黎尧), Li-Tuo Liu(刘立拓), Xiao-Mei Chen(陈晓梅), and Wei-Hu Zhou(周维虎)

Citation: Chin. Phys. B, 2021, 30 (**1**): 014206. DOI: 10.1088/1674-1056/abc153
Journal homepage: http://cpb.iphy.ac.cn; http://iopscience.iop.org/cpb

What follows is a list of articles you may be interested in

Role of quantum paths in generation of attosecond pulses

M R Sami, A Shahbaz
Chin. Phys. B, 2020, 29 (**10**): 104207. DOI: 10.1088/1674-1056/ab9deb

An improved method for the investigation of high-order harmonic generation from graphene

Zhong Guan(管仲), Lu Liu(刘璐), Guo-Li Wang(王国利), Song-Feng Zhao(赵松峰), Zhi-Hong Jiao(焦志宏), Xiao-Xin Zhou(周效信)
Chin. Phys. B, 2020, 29 (**10**): 104206. DOI: 10.1088/1674-1056/abab76

Two-dimensionally controllable DSR generation from dumbbell-shaped mode-locked all-fiber laser

Zhi-Yuan Dou(窦志远), Bin Zhang(张斌), Jun-Hao Cai(蔡君豪), Jing Hou(侯静)
Chin. Phys. B, 2020, 29 (**9**): 094201. DOI: 10.1088/1674-1056/ab9de1

Photoelectron momentum distributions of single-photon ionization under a pair of elliptically polarized attosecond laser pulses

Hui-Fang Cui(崔会芳), Xiang-Yang Miao(苗向阳)
Chin. Phys. B, 2020, 29 (**7**): 074203. DOI: 10.1088/1674-1056/ab8ac0

Self-starting all-fiber PM Er: laser mode locked by a biased nonlinear amplifying loop mirror

Ke Yin(殷科), Yi-Ming Li(李仪茗), Yan-Bin Wang(王彦斌), Xin Zheng(郑鑫), Tian Jiang(江天)
Chin. Phys. B, 2019, 28 (**12**): 124203. DOI: 10.1088/1674-1056/ab4d42

Suppression of multi-pulse formation in all-polarization-maintaining figure-9 erbium-doped fiber mode-locked laser*

Jun-Kai Shi(石俊凯)[1], Deng-Feng Dong(董登峰)[1,2,†], Ying-Ling Pan(潘映伶)[1], Guan-Nan Li(李冠楠)[1], Yao Li(黎尧)[1], Li-Tuo Liu(刘立拓)[1], Xiao-Mei Chen(陈晓梅)[1], and Wei-Hu Zhou(周维虎)[1,2]

[1] *Optoelectronic Technology R & D Center, Institute of Microelectronics, Chinese Academy of Sciences, Beijing* 100029, *China*
[2] *University of Chinese Academy of Sciences, Beijing* 100049, *China*

(Received 31 July 2020; revised manuscript received 26 August 2020; accepted manuscript online 15 October 2020)

We report on a novel architecture to suppress the multi-pulse formation in an all-polarization-maintaining figure-9 erbium-doped fiber laser under high pump power. A 2×2 fiber coupler is introduced into the phase-biased nonlinear amplifying loop mirror to extract part of intracavity laser power as a laser output, and the dependence of output couple ratio of fiber coupler on the mode-locking state is experimentally investigated. The intracavity nonlinear effect is mitigated by lowering the intracavity laser power, which is conducive to avoiding the multi-pulse formation. In the meantime, the loss-imbalance induced by fiber coupler is helpful in improving the self-starting ability. With the proposed laser structure, the multiple pulse formation can be suppressed and high power single pulse train can be obtained. The laser emits three pulse trains which is convenient for some applications. Finally, the output power values of three ports are 5.3 mW, 51.3 mW, and 13.2 mW, respectively. The total single pulse output power is 69.8 mW, which is more than 10 times the result without OC_2. The total slope efficiency is about 10.1%. The repetition rate of three pulse trains is 21.17 MHz, and the pulse widths are 2.8 ps, 2.63 ps, and 6.66 ps, respectively.

Keywords: figure-9 mode-locked fiber laser, nonlinear amplifying loop mirror, suppression of multi-pulse formation

PACS: 42.65.Re, 42.55.Wd, 42.60.Fc **DOI:** 10.1088/1674-1056/abc153

1. Introduction

In recent years, passively mode-locked erbium-doped fiber (EDF) lasers cause a large number of concerns as compact, low-cost and robust ultrashort pulse sources at 1.5-μm band for various applications ranging from industrial purposes to fundamental researches, such as spectroscopy, precision metrology, optical communication, microscopy, and material processing, to name a few.[1–3]

To realize passively mode-locked operation, various material saturable absorbers (SAs) have been widely reported, such as semiconductor saturable absorption mirror,[4,5] single-walled carbon nanotube,[6,7] graphene,[8,9] topological insulators,[10,11] and black phosphorus.[12,13] The material-based SAs often suffer thermal damage and oxidation, thus limiting the intracavity laser power and long-term stability of the fiber laser. The alternative techniques to solve the problems are the use of SAs based on fiber nonlinearity, such as nonlinear polarization evolution,[14,15] nonlinear optical loop mirror (NOLM),[16,17] nonlinear amplifying loop mirror (NALM),[18,19] Mamyshev oscillator,[20,21] and nonlinear multimode interference.[22,23] Among them, phase-biased NOLM and NALM would be favored because of fast recovery time, high damage threshold, good self-starting (SS) ability, low-cost, and the possibility of all-polarization-maintaining (PM) fiber implementation.

Moreover, passively mode-locked lasers operating with anomalous dispersion usually demonstrate multi-pulse operation under sufficient power. Different states are observed and investigated, such as bound-state solitons,[24,25] vector solitons,[26] soliton molecules,[27,28] soliton rains,[29] and dissipative soliton resonances.[30,31] But the fundamental mode-locked operation is more favorable for certain practical applications because of its intrinsic low timing-jitter and amplitude fluctuation.[32,33] When the laser operates in multi-pulse regime, the intracavity pulse number can be reduced by simply lowering the pump power. But the output power also decreases.

In this work, we propose an architecture to suppress the multi-pulse formation in an all-PM figure-9 EDF laser under high pump power. A 2×2 fiber coupler is introduced into the phase biased NALM to extract part of intracavity laser power as a laser output, so the intracavity laser power is reduced. The intracavity nonlinear effect is mitigated which is conducive to avoiding the multi-pulse formation. With this architecture, the single pulse operation can be obtained with high pump power. The laser emits three pulse trains, which is convenient for some applications. Finally, the output power values of three ports are 5.3 mW, 51.3 mW, and 13.2 mW, respectively. The

*Project supported by the National Natural Science Foundation of China (Grant No. 51905528), the Key Research Project of Bureau of Frontier Sciences and Education, Chinese Academy of Sciences (Grant No. QYZDY-SSW-JSC008), and the National Key Research and Development Project, China (Grant Nos. 2019YFB2005600 and 2018YFB2003403).

†Corresponding author. E-mail: dongdengfeng@ime.ac.cn

© 2021 Chinese Physical Society and IOP Publishing Ltd

repetition rate is 21.17 MHz, and the pulse widths are 2.8 ps, 2.63 ps, and 6.66 ps, respectively.

2. Experimental setup

The schematic experimental setup of the figure-9 laser is shown in Fig. 1. A 2×2 PM fiber optical coupler (OC_1) with a splitting ratio of 50% is used at the junction of the proposed architecture. The NALM is formed with a piece of 1-m PM EDF (PM-ESF-7/125, Nufern). The gain fiber has a mode field diameter of 8.8 μm, a core absorption of 55 dB/m at a wavelength of 1530 nm and a group velocity dispersion of -0.02 ps^2/m. A laser diode (LD) with a pump wavelength and maximum output power of 976 nm and 800 mW is employed to pump the EDF with a standard PM 976/1550 nm wavelength division multiplexer (WDM_1), and the residual pump laser is extracted out of the cavity by WDM_2. The linear arm of the figure-9 cavity consists of a high reflector (HR) and a 2-nm bandpass filter (BPF) with a center wavelength of 1550 nm. The BPF works to block the longer-wavelength (Raman self-frequency shift) and reduce the intracavity pulse duration, so the intracavity pulse can rapidly evolve back over the next roundtrip. The laser transmitting through the NALM is utilized as an output (OP_1). A home-made non-reciprocal phase shifter is inserted into the NALM. The phase shifter consists of a 45° Faraday rotator, two quarter waveplates (QWPs), and a half waveplate (HWP). Without the non-reciprocal phase shifter, the reflection of NALM for low intensity is close to a maximum value and the NALM does not offer any intensity dependence. In such a condition, ultrahigh intracavity power or ultralong fiber loop is necessary to initiate mode-locking. With the phase shifter, the NALM offers obviously intensity dependence for low intensity, and SS operation can be achieved easily. To suppress the multi-pulse formation, OC_2 is introduced and the laser beams coupled out of the cavity by OC_2 are used as a clockwise output (OP_{CW}) and counter-clockwise output (OP_{CCW}). The group velocity dispersion of the passive PM fiber is -0.022 ps^2/m, and the net cavity dispersion is estimated as -0.21 ps^2. The output laser is measured by a digital storage oscilloscope (KEYSIGHT, DSO9254A), and a radio-frequency analyzer (KEYSIGHT, N9010A) together with a 1-GHz photo detector. The spectrum is recorded by an optical spectrum analyzer (YOKOGAWA, AQ6370D), and the pulse profile is measured by a commercial autocorrelator (APE PulseCheck).

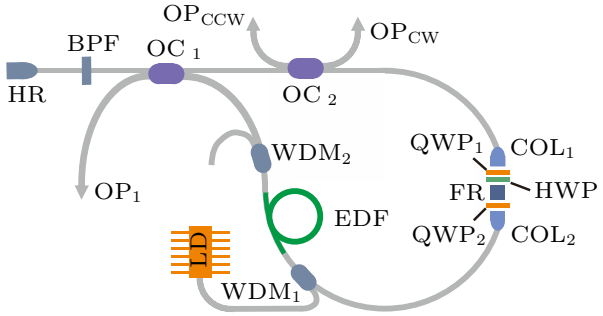


Fig. 1. Schematic diagram of experimental setup, LD: laser diode; WDM: wavelength division multiplexer; OC: optical coupler; EDF: erbium-doped fiber; BPF: bandpass filter; PS: phase shifter; HR: high reflector; OP: output; OP_{CW}: clockwise output; OP_{CCW}: counter-clockwise output; COL: collimator; FR: Faraday rotator; QWP: quarter waveplate; HWP: half waveplate.

3. Results and discussion

In our experiment, the OC_2 is replaced by a piece of passive PM fiber with almost the same length firstly. The pump power is set to be an available maximum of 750 mW, and the SS mode-locked operation is realized by finely adjusting the waveplates in the phase shifter, however, in the multi-pulse regime. The pulse trains and optical spectra for

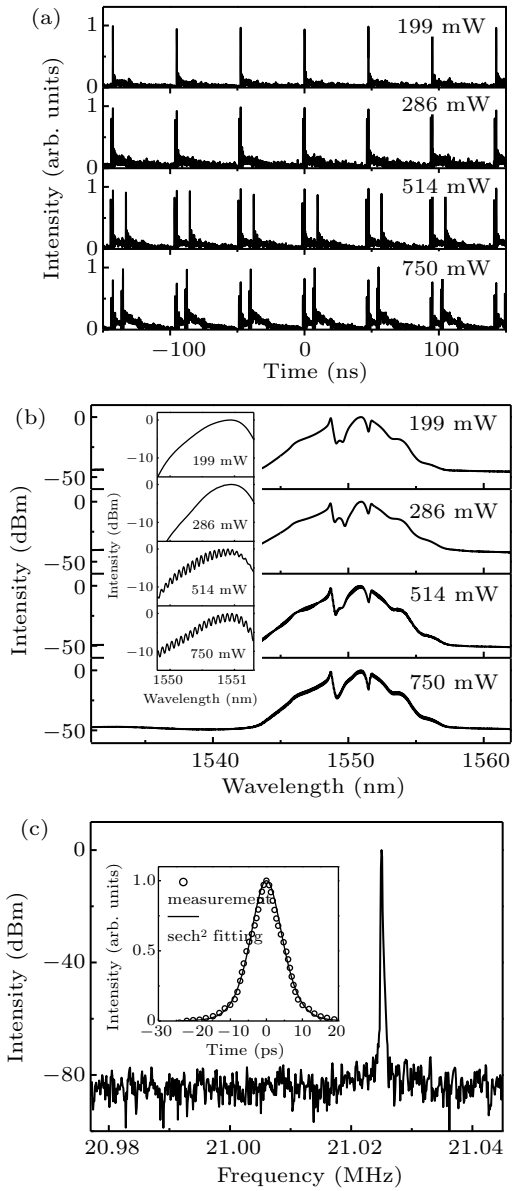


Fig. 2. Output characteristics of figure-9 mode-locked EDF laser without OC_2 showing (a) pulse trains and (b) mode-locked output spectra (inset: details around central wavelength) with different pump power values, (c) radio-frequency spectrum (inset: autocorrelation trace) of single pulse output.

different pump power values are shown in Figs. 2(a) and 2(b). The laser operates in four-pulse regime with pump power of 750 mW, and the output power is 30 mW. As shown in Fig. 2(b), there are some dips in the spectrum which are induced by the interference of the counter-propagated pulses at the OP_1 port. The inset of Fig. 2(b) shows the spectral details with a resolution of 0.01 nm around the central wavelength. The spectrum is modulated with a period of 0.07 nm which proves the operation of bound state solitons. As the pump power decreases, the laser turns into three-, two- and single-pulse operations at the pump power values of 514, 289, and 199 mW, respectively, and the interference pattern of spectrum finally vanishes. The temporal traces of mode-locked pulses show up obvious noise on the substrates, which is mainly attributed to the intrinsic noise of oscilloscope and photo detector. Figure 2(c) shows the radio-frequency (RF) spectrum of single-pulse output with a resolution bandwidth (RBW) of 100 Hz, and the inset shows the autocorrelation trace. The repetition rate is 21.025 MHz, which accords well with the periods of the pulse trains. The full width at half-maximum (FWHM) of autocorrelation trace is 10.96 ps, and the corresponding pulse width is estimated at 7.12 ps under a sech^2-shape assumption. The signal-to-noise ratio (SNR) of 73.6 dB indicates the excellent stability of the soliton mode-locked opetation. The single-pulse operation can be realized by reducing the pump power, but it is inconvenient for use, and the output power is as low as 6 mW.

To overcome the drawbacks mentioned above, an OC_2 is inserted into the NALM. The OC_2 works as both power attenuator and bidirectional output coupler. Part of the intracavity laser power is extracted as a laser output, and the intracavity nonlinear effect is mitigated, which is conducive to avoiding the multi-pulse formation. In the meantime, the loss-imbalance induced by OC_2 is helpful in improving the SS ability.[34] The dependence of output couple ratio of OC_2 on the mode-locking state is investigated to confirm the significance of the proposed architecture, and the mode-locking output characteristics versus 750-mW pump power are shown in Fig. 3. The repetition rate remains around 21 MHz with different output ratios as shown in Fig. 3(a), and the SNR remains above 70 dB. When the output couple ratio is increased from 0% to 60%, the number of circulating pulses gradually decreases and single pulse operation finally is achieved as shown in Fig. 3(b). It can be understood as the higher output couple ratio leading to lower intracavity power and consequent weaker self-phase modulation, which is conducive to avoiding wave-breaking. The result shows that the SS single pulse operation can be realized easily with an output ratio of 50% or greater. Figure 3(c) shows that the mode-locking threshold and loss of locking threshold exponentially increase as the output ratio increases, which is attributed to larger cavity loss. The mode-locking threshold with an output ratio of 70% or greater is higher than the available maximum pump power, so the mode-locking cannot be achieved. Figure 3(d) shows the output power values of three ports for different output couple ratios. The power values of OP_{CW} and OP_{CCW} increase with the increase of output couple ratio, especially for OP_{CCW} which increases from 0 mW to 51 mW with the output couple ratio increasing from 0% to 60%. Although the power of OP_1 decreases, the total output power increases significantly.

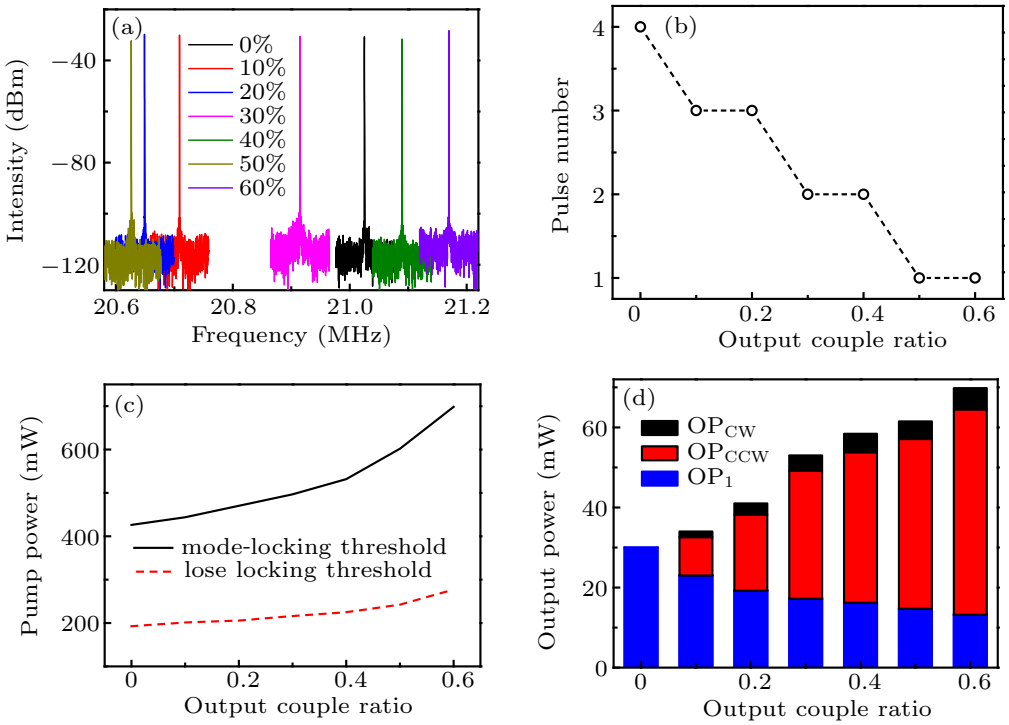


Fig. 3. Experimentally observed mode-locked (a) RF spectra, (b) intracavity pulse number, (c) mode-locking threshold and lose locking threshold, (d) output power values *versus* output couple ratio under pump power of 750 mW for different OP cases.

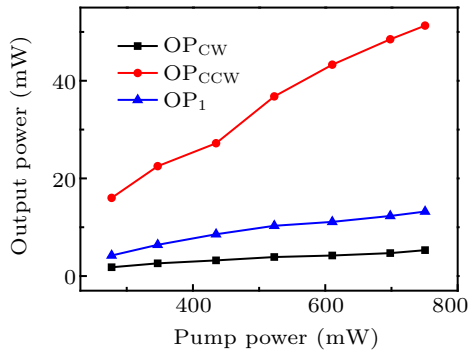


Fig. 4. Plots of output power *versus* pump power with output couple ratio of 60% for different OP cases.

With an output couple ratio of 60%, the figure-9 mode-locked EDF laser works in single-pulse state under the pump power of 750 mW. The output power values of three ports for different pump power values are shown in Fig. 4. The maximum output power values of OP_{CW}, OP_{CCW}, and OP_1 are 5.3 mW, 51.3 mW, and 13.2 mW, respectively. The total single pulse output power is 69.8 mW, which is more than 10 times the result without OC_2. The total slope efficiency is about 10.1%. Figures 5(a) and 5(b) present the optical spectra and autocorrelation traces of the pulses emitted from OP_{CW}, OP_{CCW}, and OP_1, and the inset of Fig. 5(a) shows the spectral details around central wavelength. The FWHMs of autocorrelation traces are 4.32 ps, 4.05 ps, and 10.25ps, and the pulse durations are estimated at 2.8 ps, 2.63 ps, and 6.66 ps with a sech^2-shape assumption, respectively. The 3-dB spectral bandwidths are 2.58 nm, 3.24 nm, and 3.33 nm, with the corresponding time-bandwidth products of 0.903, 1.063, and 2.765, respectively. The OP_{CW} pulse can be considered as an NALM input pulse, because it exits shortly after entering the fiber loop. The spectral sideband of OP_{CW} is removed by the BPF. The OP_{CCW} pulse can be considered as an NALM output pulse, the distortion is caused by nonlinear chirp accumulation during amplification and transmission in the passive fiber. The OP_1 pulse can be considered as the superposition of CW and CCW output pulses of the NALM. These two pulses experience passive fiber, phase shifter and gain fiber in the opposite order and direction. As a consequence, there is a phase delay difference and a slightly time delay between the counter-propagating pulses, and OP_1 pulse duration is much larger than the other output pulses. The pulse trains are shown in Fig. 5(c). The period of the pulse trains is about 47.24 ns, which accords well with the cavity roundtrip time and confirms the mode-locked operation. The RF spectra around the fundamental repetition rate are measured with an RBW of 100 Hz as shown in Fig. 5(d), and the RF spectra measured in a range of 1 GHz are shown in the inset of Fig. 5(d). The fundamental repetition rate is 21.17 MHz, which matches with the period of the pulse trains. The SNRs of 72 dB demonstrate the good stability of the soliton mode-locked operation. The experimental results indicate that the proposed architecture can effectively suppress multi-pulse formation in a figure-9 ultrafast laser, and significantly improve the single pulse output power.

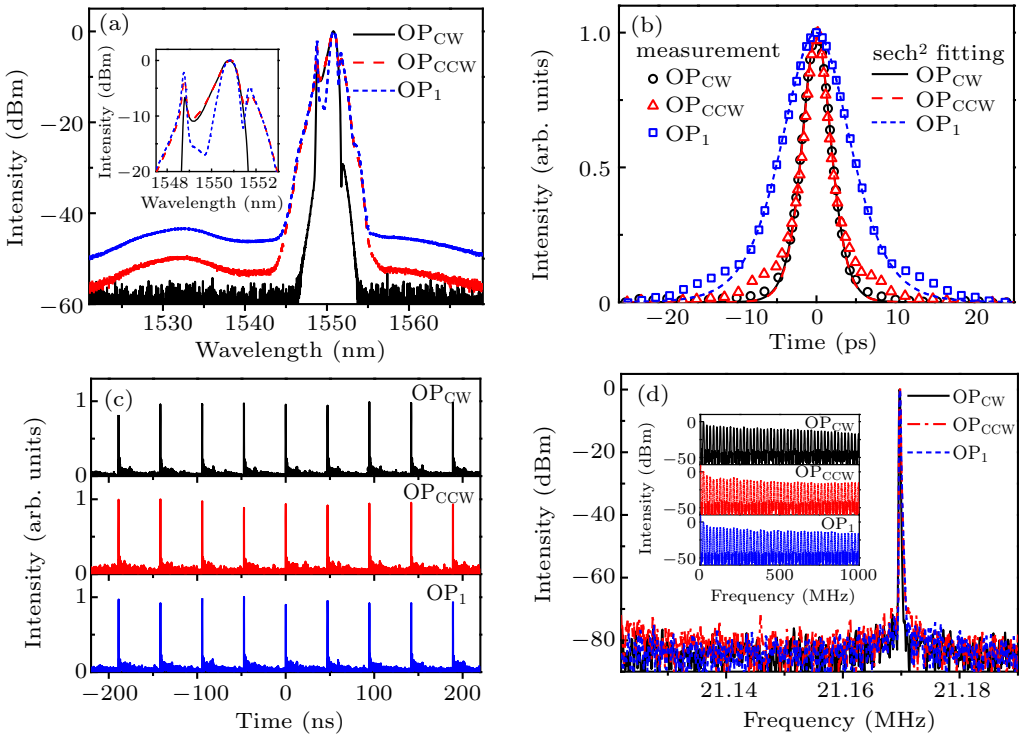


Fig. 5. (a) Output spectra (inset: spectra in details), (b) autocorrelation traces, (c) pulse trains, and (d) RF spectra over a 70-kHz span with 100-Hz resolution (inset: RF spectra in large domain) with output couple ratio of 60% and pump power of 750 mW.

4. Conclusions

In this work, an all-PM figure-9 EDF laser is experimentally investigated. A bidirectional OC is introduced into the NALM to suppress multiple pulse formation and improve the output power of single pulse train. The SS mode-locked operation is realized easily. The influence of output ratio of OC_2 on the output characteristics is experimentally investigated, and the pulse evolution in the figure-9 cavity is also studied. Finally, the output power values of three ports are 5.3 mW, 51.3 mW, and 13.2 mW, respectively. The total single pulse output power is 69.8 mW, which is more than 10 times the result without OC_2. This setup provides three pulse trains, which can be useful for applications.

References

[1] Shi J K and Zhou W H 2018 *Chin. Opt. Lett.* **16** 031404
[2] Zhao X, Zheng Z, Liu L, Liu Y, Jiang Y X, Yang X and Zhu J S 2011 *Opt. Express* **19** 1168
[3] Huang S S, Wang Y G, Yan P G, Zhao J Q, Li H Q and Lin R Y 2015 *Opt. Express* **22** 11417
[4] Lian F Q, Fan Z W, Bai Z N, Li X H and Wang Q J 2015 *Photon. Res.* **3** 129
[5] Armas-Rivera I, Cuadrado-Laborde C, Carrascosa A, Kuzin E A, Beltran-Perez G, Diez A and Andres M V 2016 *Opt. Express* **24** 9966
[6] Hou L, Guo H Y, Wang Y G, Sun J, Lin Q M, Bai Y and Bai J T 2018 *Opt. Express* **26** 9063
[7] Han X X 2018 *Appl. Opt.* **57** 807
[8] Boguslawski J, Sotor J, Sobon G, Kozinski R, Librant K, Aksienionek M, Lipinska L and Abramski K 2015 *Photon. Res.* **3** 119
[9] Zhu G W, Zhu X S, Wang F Q, Xu S, Li Y, Guo X L, Balakrishnan K, Norwood R and Peyghambarian N 2016 *IEEE Photon. Technol. Lett.* **28** 7
[10] Li L, Su Y L, Wang Y G, Wang X, Wang Y S, Li X H, Mao D and Si J H 2017 *IEEE J. Sel. Top. Quantum Electron.* **23** 1
[11] Wang J T, Jiang Z K, Chen H, Li J R, Yin J D, Wang J Z, He T C, Yan P G and Ruan S C 2018 *Photon. Res.* **6** 535
[12] Chen Y, Chen S Q, Liu J, Gao Y X and Zhang W J 2016 *Opt. Express* **24** 13316
[13] Hisyam M B, Rusdi M F M, Latiff A A and Harun S W 2017 *IEEE J. Sel. Top. Quantum Electron.* **23** 39
[14] Zhang J, Kong Z Y, Liu Y Z, Wang A M and Zhang Z G 2016 *Photon. Res.* **4** 27
[15] Kuang Q Q, Zhan L, Gu Z C and Wang Z Q 2015 *J. Lightwave Technol.* **33** 391
[16] Szczepanek J, Kardas T M, Michalska M, Radzewicz C and Stepanenko Y 2015 *Opt. Lett.* **40** 3500
[17] Aleshkina S S, Bubnov M M, Senatorov A K, Lipatov D S and Likhachev M E 2016 *Laser Phys. Lett.* **13** 035104
[18] Liu W, Shi H S, Cui J H, Xie C, Song Y J, Wang C Y and Hu M L 2018 *Opt. Lett.* **43** 2848
[19] Liu G Y, Wang A M and Zhang Z G 2017 *IEEE Photon. Technol. Lett.* **29** 2055
[20] Liu Z W, Ziegler Z M, Wright L G and Wise F W 2017 *Optica* **4** 649
[21] Liu W, Liao R Y, Zhao J, Cui J H, Song Y J, Wang C Y and Hu M L 2019 *Optica* **6** 194
[22] Wang Z K, Wang D N, Yang F, Li L J, Zhao C L, Xu B, Jin S Z, Cao S Y and Fang Z J 2018 *Opt. Lett.* **43** 2078
[23] Tegin U and Ortac B 2018 *Opt. Lett.* **43** 1611
[24] Wang Z T, Xu Y H, Dhanabalan S C, Sophia J, Zhao C J, Xu C W, Xiang Y J, Li J Q and Zhang H 2016 *IEEE Photon. J.* **7** 1503310
[25] Chen Y, Wu M, Tang P H, Chen S Q, Du J, Jiang G B, Li Y, Zhao C J, Zhang H and Wen S C 2014 *Laser Phys. Lett.* **11** 055101
[26] Song Y, Chen S, Zhang Q, Li L, Zhao L, Zhang H and Tang D 2016 *Opt. Express* **24** 25933
[27] Luo A P, Zhu P F, Liu H, Zheng X W, Zhao N, Liu M, Cui H, Luo Z C and Xu W C 2014 *Opt. Express* **22** 27019
[28] Liu X M, Yao X K and Cui Y D 2018 *Phys. Rev. Lett.* **121** 023905
[29] Chouli S and Grelu P 2009 *Opt. Express* **17** 11776
[30] Chang W, Ankiewicz A, Soto-Crespo J M and Akhmediev N 2008 *Phys. Rev. A* **78** 023830
[31] Wu X, Tang D Y, Zhang H and Zhao L M 2009 *Opt. Express* **17** 5580
[32] Zhou Y, Lin W, Cheng H H, Wang W L, Qiao T, Qian Q, Xu S H and Yang Z M 2018 *Opt. Express* **26** 10842
[33] Zhao J Q, Li L, Zhao L M, Tang D Y, Shen D Y and Su L 2019 *Photon. Res.* **7** 332
[34] Shi J K, Li Y, Gao S Y, Pan Y L, Wang G M, Ji R Y and Zhou W H 2018 *Chin. Opt. Lett.* **16** 121404